

## Article

# Activated Carbons for Syngas Desulfurization: Evaluating Approaches for Enhancing Low-Temperature H<sub>2</sub>S Oxidation Rate

Christian Frilund \* , Ilkka Hiltunen and Pekka Simell 

VTT Technical Research Centre of Finland Ltd., P.O. Box 1000, FI-02044 Espoo, Finland; ilkka.hiltunen@vtt.fi (I.H.); pekka.simell@vtt.fi (P.S.)

\* Correspondence: christian.frilund@vtt.fi

**Abstract:** Its relatively low cost and high surface area makes activated carbon an ideal adsorbent candidate for H<sub>2</sub>S removal. However, physical adsorption of H<sub>2</sub>S is not very effective; therefore, methods to facilitate reactive H<sub>2</sub>S oxidation on carbons are of interest. The performance of H<sub>2</sub>S removal of non-impregnated, impregnated, and doped activated carbon in low-temperature syngas was evaluated in fixed-bed breakthrough tests. The importance of oxygen content and relative humidity was established for reactive H<sub>2</sub>S removal. Impregnates especially improved the adsorption rate compared to non-impregnated carbons. Non-impregnated carbons could however retain a high capture capacity with sufficient contact time. In a relative performance test, the best performance was achieved by doped activated carbon, 320 mg g<sup>-1</sup>. Ammonia in syngas was found to significantly improve the adsorption rate of non-impregnated activated carbon. A small quantity of ammonia was consumed by the carbon bed, suggesting that ammonia is a reactant. Finally, to validate ammonia-enhanced desulfurization, bench-scale experiments were performed in biomass-based gasification syngas. The results show that when the ammonia concentration in syngas was in the tens of ppm range, 40–160 ppm H<sub>2</sub>S oxidation proceeded rapidly. Ammonia-enhanced oxidation allows utilization of cheaper non-impregnated activated carbons by in situ improvement of the adsorption kinetics. Ammonia enhancement is therefore established as a viable method for achieving high-capacity H<sub>2</sub>S removal with unmodified activated carbons.

**Keywords:** syngas desulfurization; activated carbon; hydrogen sulfide; H<sub>2</sub>S oxidation; ammonia



**Citation:** Frilund, C.; Hiltunen, I.; Simell, P. Activated Carbons for Syngas Desulfurization: Evaluating Approaches for Enhancing Low-Temperature H<sub>2</sub>S Oxidation Rate. *ChemEngineering* **2021**, *5*, 23. <https://doi.org/10.3390/chemengineering5020023>

Academic Editor: Martín Ramirez

Received: 17 March 2021

Accepted: 6 May 2021

Published: 11 May 2021

**Publisher's Note:** MDPI stays neutral with regard to jurisdictional claims in published maps and institutional affiliations.



**Copyright:** © 2021 by the authors. Licensee MDPI, Basel, Switzerland. This article is an open access article distributed under the terms and conditions of the Creative Commons Attribution (CC BY) license (<https://creativecommons.org/licenses/by/4.0/>).

## 1. Introduction

Sulfur exists naturally in most industrially utilized hydrocarbon sources, e.g., crude oil, natural- and biogas, and biomass. Gasification of biomass is an interesting platform for the sustainable production of synthetic chemicals and fuels. The requirements for sulfur removal are particularly stringent for catalytic synthesis and therefore effective, robust and low-cost syngas cleaning solutions are crucial.

H<sub>2</sub>S removal methods vary by application and are commonly based on physicochemical phenomena such as reactive conversion, absorption, or adsorption. For high acid gas concentrations and large-scale processing, absorptive removal has been the most utilized and economical route [1]. Adsorption processes, due to their simplicity and mild operating conditions, can potentially be used for very economical and deep removal of sulfur gases, especially at a smaller scale. Activated carbons are amorphous carbon materials with a surface area up to thousands of square meters per gram and a well-developed microporosity [2]. They are widely used for processing industrial gases [3–5], air [6–8], and waste water purification [9] due to their versatile nature as adsorbents or catalysts and their multi-pollutant removal capability [10]. Other than surface area, pore volume, and pore size distribution, it is known that altering the surface functional groups present

on the carbon, for example by changing the pH, greatly affect the adsorption or reaction mechanism of H<sub>2</sub>S and thus the removal performance [11].

The relatively low cost of activated carbons compared to other desulfurization adsorbents, such as inorganic materials (e.g., metal oxides), makes it an attractive adsorbent candidate. In dry and oxygen lacking conditions, only weak and reversible physical adsorption of H<sub>2</sub>S has been demonstrated to occur [10,12,13]. Therefore, methods to facilitate faster reactions between the surface and the adsorbate have generated much research interest. The most common way to improve the rate of H<sub>2</sub>S adsorption has been to impregnate the surface with basic compounds such as NaOH or KOH or oxidative agents such as KI [14]. It has been shown that when operating with more diverse gas mixtures, chemical adsorption is unavoidable due to interactions between the gas and functional groups, making H<sub>2</sub>S removal on activated carbons a complex phenomenon [15]. The presence of oxygen and moisture facilitating the H<sub>2</sub>S oxidation reaction has been shown to improve uptake and is thus crucial for fast and effective removal of sulfur [11,16,17]. Reports of gaseous ammonia improving the desulfurization rate also exist [18,19].

Herein, we report the H<sub>2</sub>S removal performance of different types of commercial activated carbons in a syngas atmosphere in a dynamic fixed-bed reactor arrangement. The influence of key parameters on oxidative desulfurization, including gas relative humidity and gas composition in terms of oxygen and ammonia content, was investigated to evaluate the best conditions for a continuous, kinetically fast sulfur adsorption process for biomass-derived syngas. Finally, the best lab-scale derived conditions were validated in real syngas in bench-scale desulfurization experiments.

## 2. Materials and Methods

### 2.1. Adsorbent Materials

Four commercial pelletized activated carbon adsorbents were tested at lab scale to assess their performance for H<sub>2</sub>S removal in syngas. These activated carbons, listed in Table 1, had different material properties and thus varying bases for sulfur adsorption.

**Table 1.** Activated carbon materials and their measured density, specific surface area, pore volume, and surface pH.

Name	Material Type	Density <sup>1</sup> (m <sup>2</sup> g <sup>-1</sup> )	BET-SA (m <sup>2</sup> g <sup>-1</sup> )	V <sub>mic</sub> (cm <sup>3</sup> g <sup>-1</sup> )	V <sub>mes</sub> (cm <sup>3</sup> g <sup>-1</sup> )	pH
AC1	Non-impregnated activated carbon	0.43	520	0.13	0.28	10.8
AC2	Non-impregnated activated carbon	0.39	1000	0.35	0.11	10.1
IAC	KI impregnated activated carbon	0.45	980	0.37	0.05	n.a.
DAC	Doped activated carbon	0.36	880	0.32	0.04	10.4

<sup>1</sup> Packed reactor 1 for 0.5–0.85 mm particle size distribution.

AC1, virgin non-impregnated activated carbon, was supplied by Cabot under the name Darco BG1, which is especially utilized for biogas H<sub>2</sub>S removal and has well-developed mesoporosity. AC2 was a virgin non-impregnated activated carbon with high microporosity, supplied by Jacobi Carbons (AddSorb Sulfox), also utilized for H<sub>2</sub>S removal. IAC was a KI impregnated carbon by Cabot (Norit ROZ3). DAC was supplied by AdFis, dopetac sulfo 100<sup>®</sup>, and was a doped activated carbon for H<sub>2</sub>S removal. Tested materials were crushed and sieved to desired size distribution: 0.3–1.0 mm, 0.5–0.85 mm, or 1.0–1.25 mm depending on the experiment.

### 2.2. Methods

#### 2.2.1. Lab-Scale Desulfurization

The laboratory-scale breakthrough capacity tests were performed in atmospheric quartz packed-bed reactors. External heating was applied to achieve a bed temperature of 50 ± 3 °C. The gases were dosed using Bronkhorst mass flow controllers, and in experiments with a set relative moisture content, water was fed to an evaporator. The model syngas was inspired by typical biomass-based fluidized bed gasification syngas with

a volume-based dry composition of H<sub>2</sub> 53.5%, CO 26.7%, CO<sub>2</sub> 19.0%, and CH<sub>4</sub> 0.8%. The water feed rate was calculated for 50% relative humidity to equal around 6.5%, derived from water vapor pressure at 50 °C. In this study, small gas concentrations are reported as parts per million (ppm) in volume terms (cm<sup>3</sup> m<sup>-3</sup>). H<sub>2</sub>S concentration varied between 70 and 280 ppm in dry gas, which is equivalent to a low to medium sulfur concentration of gasification syngas. In experimental points with added oxygen, the concentration was fixed to 3000 ppm (dry basis). NH<sub>3</sub> addition in select experiments was fixed to a concentration of 35 ppm. The bottled gases were mixed with the vaporized water in a heated inlet line. The effluent gas was cooled in a condenser tube with a cooling water jacket.

Two reactor scales were used to investigate the space velocity effect on adsorption dynamics. In this study, space velocity (SV) is reported in volume terms under standard conditions, defined as 273.15 K and 101.325 kPa. The inner diameter of reactor 1 was 1.5 cm, with a thermocouple pocket 0.4 cm in diameter at the center of the bed. The effective adsorbent volume at a standard bed height of 4.5 cm (height-to-diameter ratio of 3) was thus 7.4 cm<sup>3</sup>. The inner diameter of reactor 2 was 2.6 cm. Reactor 2 did not have a thermocouple pocket, thus with a 6 cm bed height the effective reactor volume was 32.7 cm<sup>3</sup> (height-to-diameter ratio of 2.3). The total gas flow rate was either 2 or 3 dm<sup>3</sup> min<sup>-1</sup> depending on the experiment. All gas volumes in this study are expressed in standard conditions.

The sulfur adsorption capacity is the sulfur captured per mass of adsorbent at a given breakthrough, and is given according to:

$$S_{cap} = \frac{t_b \cdot \dot{V}_g \cdot c_{H_2S} \cdot M_S}{V_{mol} \cdot m_{ads}} \quad (1)$$

where  $S_{cap}$  is the sulfur adsorption capacity (mg g<sup>-1</sup>),  $t_b$  is the breakthrough time (min),  $\dot{V}_g$  is the total gas flow rate (dm<sup>3</sup> min<sup>-1</sup>),  $c_{H_2S}$  is the H<sub>2</sub>S concentration (ppm),  $M_S$  is the molar mass of sulfur,  $V_{mol}$  is the molar volume, and  $m_{ads}$  is the adsorbent weight (g).

For lab-scale tests, a breakthrough limit of 2 ppm H<sub>2</sub>S in the effluent was chosen, which is equivalent to 0.7–3% of H<sub>2</sub>S feed concentration, depending on the experiment. Breakthrough times were estimated using polynomial interpolation. H<sub>2</sub>S concentration is reported in dry syngas.

The breakthrough capacity was determined from the experiments by non-interrupted operation that was generally stopped after the breakthrough limit was achieved, when a sharp breakthrough was detected.

### 2.2.2. Bench-Scale Desulfurization

A bench-scale adsorption test rig was connected to a gasifier with biomass feedstock. The gasification facility consisted of a bubbling fluidized bed (BFB), a hot filtration unit, and a reformer unit (Ni-based catalyst) [20]. The modified bench-scale unit [21], shown in Figure 1, was connected to the reformer slipstream.

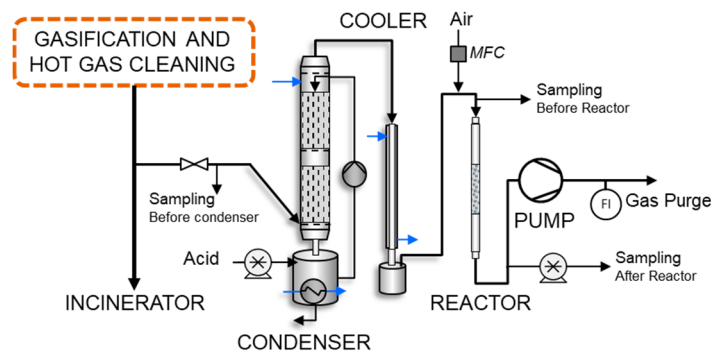


**Figure 1.** Schematic illustration of bench-scale fixed-bed adsorption unit connected to gasification facility slipstream consisting of a condenser, cooler, adsorbent reactor, and pump.

The bench-scale system consisted of the following units: (1) water scrubbing column with optional formic acid and fresh water feeding, (2) jacketed water cooling tube for gas temperature control, (3) metallic packed-bed reactor with flow distributor before the bed, (4) Masterflex peristaltic pump, and (5) flow meter (pressure-difference method).

The main gas composition before the condenser of the bench-scale unit is given in Table 2.

**Table 2.** Average GC-derived gas composition before bench-scale test rig (post-reformer).

	Sunflower Husk	Olive Tree Pruning	Straw
Feedstock S-content (%) <sup>1</sup>	0.14	0.08	0.11
CO (%)	20.7	22.0	18.4
H <sub>2</sub> (%)	40.0	40.6	38.1
CO <sub>2</sub> (%)	24.7	18.8	21.8
CH <sub>4</sub> (%)	1.7	2.1	2.4
N <sub>2</sub> (%)	12.8	16.5	19.3
Benzene and tars (mg m <sup>-3</sup> ) <sup>2</sup>	70	70	180
NH <sub>3</sub> (ppm) <sup>2</sup>	260	770	460

<sup>1</sup> Dry basis in mass fractions; <sup>2</sup> offline sampling.

Ammonia concentration in the gas for the AC reactor was adjusted with the condenser unit. Full removal of ammonia was achieved by adjusting the closed-loop water circulation to pH 3, and partial removal (>90 %) was achieved by fresh water (pH 7–8) scrubbing of the gas. Full concentration of ammonia in the raw syngas according to Table 2 was preserved by bypassing the water scrubbing step completely. Moisture content was set to below saturation point, and the reactor was operated without external heating at 16–18 °C. The estimated gas relative humidity was 80–95% in the reactor step. Oxygen was dosed with a mass flow controller to the syngas before the reactor at a constant rate of 0.1 dm<sup>3</sup> min<sup>-1</sup>, thus the total oxygen concentration in the bench-scale experiments was in the range of 1000–2000 ppm.

The 2.54 cm i.d. reactor was filled with 15 cm adsorbent (height-to-diameter ratio of 6.0). The pump's rpm was kept constant, calibrated in nitrogen atmosphere and corrected for the experiment-specific average syngas composition. The reactor packed volume was 76 cm<sup>3</sup>. The pump suction rate was around 20 dm<sup>3</sup> min<sup>-1</sup>, with slight variations depending on the gas composition.

For bench-scale tests, a higher 10 ppm breakthrough limit was chosen, and sulfur mass flow below the breakthrough curve was accounted for in the sulfur capture capacity calculations.

### 2.3. Analytics

#### 2.3.1. Lab-Scale Gas Analytics

For lab-scale H<sub>2</sub>S concentration measurement at the reactor exit Dräger test tubes, quantitative colorimetric chemical sensors were utilized that react with H<sub>2</sub>S to form HgS, of type H<sub>2</sub>S 0.2/a (0.2–6 ppm), 2/a (2–200 ppm), and 100/a (100–2000 ppm). The reported standard deviation of this analysis method is ±5–10%, and the breakthrough curve error bars are reported as 7.5%. Sampling was performed from cooled gas after the condenser operated at 15 °C. An online gas analyzer (ABB) was used for continuous analysis of the exit dry gas composition. H<sub>2</sub>O and NH<sub>3</sub> concentrations in the reactor exit were obtained from Fourier-transform infrared spectroscopy (FTIR) spectra using a Gasetmet DX4000 analyzer. The component reference ranges were as follows: NH<sub>3</sub> 20–120 ppm and H<sub>2</sub>O 0.1–50%.

#### 2.3.2. Bench-Scale Gas Analytics

Bench-scale experiments used Dräger tubes for H<sub>2</sub>S detection, and in the final experiment an Agilent 7890A gas chromatograph with a flame photometric detector (FPD-GC) and a GS-GasPro 30 m × 0.32 mm i.d. column using He as carrier gas were used. The GC was calibrated using a calibration gas containing H<sub>2</sub>S and COS with concentrations of 200

and 20.1 ppm, respectively, with relative error of  $\pm 2\%$ . The sampling location for the feed gas was after the condenser and the effluent sampling location was directly after the reactor. An online gas analyzer was used for continuous analysis of the exit dry gas composition. In the final experiment, ammonia was analyzed from offline samples. A known gas quantity was injected to a water sample and titrated with HCl for  $\text{NH}_3$  determination.

### 2.3.3. Adsorbent Characterization

#### Adsorbent Surface pH

A total of 0.5 g of crushed activated carbon sample was mixed with 50  $\text{cm}^3$  RO water and mechanically stirred for 2 h. The suspension was allowed to stand overnight at room temperature and then was measured with a pH meter, using pH 7 and 10 buffers for  $\text{pH} > 7$  samples and pH 4 and 7 buffers for  $\text{pH} < 7$  samples.

#### $\text{N}_2$ Adsorption/Desorption

Fresh and spent activated carbons were measured at  $-196\text{ }^\circ\text{C}$  using a Micrometrics 3Flex analyzer with  $\text{N}_2$  adsorption and desorption isotherms. Samples were pre-dried at  $120\text{ }^\circ\text{C}$ . All measured activated carbon samples displayed IUPAC type 1 isotherms [22]. For specific surface area determination, the multipoint Brunauer–Emmett–Teller (BET) equation was utilized. Pore volume was estimated by the Barrett–Joyner–Halenda (BJH) method in the distribution range of micropores  $< 2.03\text{ nm}$  and mesopores  $2.03\text{--}40.8\text{ nm}$ .

#### Thermal Analysis

Thermal analysis was performed using a thermogravimeter. Sample heating rate was  $10\text{ }^\circ\text{C min}^{-1}$  at atmospheric pressure in a  $1\text{ dm}^3\text{ min}^{-1}\text{ N}_2$  stream. The sample size was in the 150 mg range. Sample was preheated at slightly above  $100\text{ }^\circ\text{C}$  to release water and other weakly bound compounds before temperature programmed heating was initialized in the range of  $125\text{--}800\text{ }^\circ\text{C}$ .

#### Elemental Analysis

Surface compositions of the samples were determined by energy dispersive X-ray spectroscopy (EDS). A Carl-Zeiss Merlin scanning electron microscope (SEM) was equipped with a Thermo Fisher UltraDry energy-dispersive X-ray spectrometer (silicon drift detector). Samples were pre-vacuumed and placed in Al stubs for imaging.

C, H, N, and S elemental composition was determined using a Thermo Fisher combustion analyzer (2.5 mg samples).

## 3. Results

### 3.1. Effect of Oxygen and Moisture Content

To assess the effect of oxygen and moisture content on  $\text{H}_2\text{S}$  capture, three accelerated breakthrough experiments were performed at lab scale ( $24,000\text{ h}^{-1}$ ) with a syngas mixture using KI impregnated activated carbon (IAC). The breakthrough results with  $\text{H}_2\text{S}$  exit concentration as a function of time on stream (TOS) are presented in Figure 2.

In the pure syngas atmosphere, the breakthrough was almost instantaneous. Moisture in the oxygen-free syngas slightly prolonged  $\text{H}_2\text{S}$  breakthrough, but a major relative improvement in  $\text{H}_2\text{S}$  capture was achieved with co-feeding of oxygen and  $\text{H}_2\text{O}$ , achieving  $20\text{ mg g}^{-1}$  capacity. The absolute performance in all tested atmospheres was low, which can be attributed to the high space velocity.

The effect of gas moisture on  $\text{H}_2\text{S}$  uptake is explained by water adsorption and capillary condensation in the pores. This forms a water film in the internal surface of the activated carbon, which improves the  $\text{H}_2\text{S}$  dissociation (first dissociation constant  $\text{pK}_{\text{a}1}$  ca. 7) in which the formed ion readily further reacts, therefore improving the  $\text{H}_2\text{S}$  reaction rate and carbon capture capacity [12,23,24]. The first  $\text{H}_2\text{S}$  dissociation can be described by Reaction (2):



An increase from low relative humidity (RH < 20%) has been shown to improve the reaction rate significantly, whereas beyond an already high relative humidity (RH > 75%), diminishing improvement has been previously reported [25].

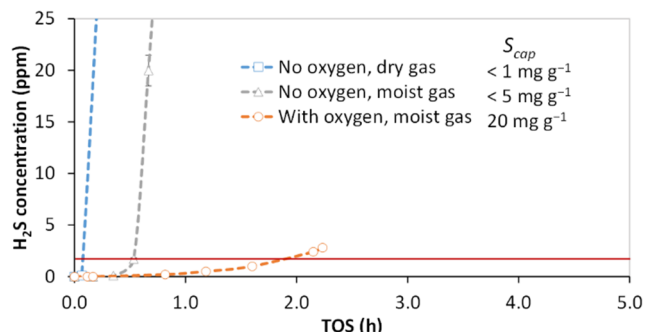


**Figure 2.** Effect of oxygen and moisture on H<sub>2</sub>S breakthrough with adsorbent impregnated activated carbon (IAC) at a space velocity (SV) of 24,000 h<sup>-1</sup> (reactor 1) and H<sub>2</sub>S feed concentration of 100 ppm at 50 °C. Capture capacity,  $S_{cap}$ , is indicated as milligrams of sulfur per gram of adsorbent. When oxygen was present the concentration was 3000 ppm, and at moist conditions relative humidity (RH) was set to 50%. Particle size distribution—1.0–1.25 mm. The horizontal red line indicates the breakthrough limit.

Oxygen has been shown to improve the H<sub>2</sub>S capture rate with both non-impregnated and impregnated carbons, suggesting similar oxidation mechanisms for both [23]. Li et al. [10] studied the oxidation mechanisms of H<sub>2</sub>S at 150 °C on virgin activated carbon and concluded that in the absence of O<sub>2</sub>, the desulfurization performance will be much lower and the H<sub>2</sub>S will be adsorbed to form sulfate. In the presence of O<sub>2</sub>, elemental sulfur was formed according to Reaction (3) [26]:



where  $x$  can be 2, 6, or 8 depending on the temperature of the reaction [27]. According to Steijns et al. [28,29] the sulfur that deposits in porous materials (AC, zeolites, alumina) in fact causes an autocatalytic effect for the oxidation of hydrogen sulfide by molecular oxygen. The reaction order with respect to H<sub>2</sub>S varies by study from 0.4 to 1.0 at the tested elevated temperatures, and the activation energy is higher in the low temperature range [30].

H<sub>2</sub>S could further react to form SO<sub>2</sub>, as described by Reaction (4) [30]:



It has been reported that at high temperatures, especially above 300 °C, the reaction rate for SO<sub>2</sub> formation is high [29]. Elemental sulfur conversion back to gaseous COS or SO<sub>2</sub> at high-temperatures has also been reported [27].

The exothermic H<sub>2</sub>S oxidation reaction is highly favorable for sulfur removal from a thermodynamic equilibrium standpoint; however, it is not very useful for sulfur removal if H<sub>2</sub>S is simultaneously converted to other gaseous sulfur compounds. Evidence reported in the literature suggests that a higher oxygen concentration, even above the stoichiometric ratio, will improve sulfur uptake [11,16]. To prevent over-oxidation of H<sub>2</sub>S to SO<sub>2</sub> according to Reaction (4), and to ensure deposition of the formed elemental sulfur in the pores, sub-100 °C reaction temperatures are required [28]. Generally, lower temperatures improve the adsorption of species and are therefore preferred [31,32]. Oxidation of H<sub>2</sub>S significantly improves H<sub>2</sub>S uptake compared with purely physical adsorption and should be the go-to route for efficient desulfurization using activated carbons. The oxidative route for H<sub>2</sub>S conversion has been utilized in industry for high-sulfur-content streams as a replacement for or complementary to the Claus-type sulfur recovery process. A metal- or carbon-based catalyst is used at elevated temperature, above the sulfur dew point, in a continuous

process to convert  $\text{H}_2\text{S}$  to elemental sulfur, followed by a separation step for condensation of sulfur [25].

Syngas is generated in oxygen-starved conditions in, e.g., coal or biomass gasification. Since downstream applications might not tolerate oxygen, the benefits of oxygen injection in the desulfurization step must justify the additional cost of downstream oxygen removal.

### 3.2. Adsorbent Relative Desulfurization Performance

Relative performance experiments were conducted in oxygen containing and moist conditions to facilitate  $\text{H}_2\text{S}$  oxidation. The effect of sulfur concentration on removal was first tested with the IAC and AC1. The breakthrough results are given in Figure 3.

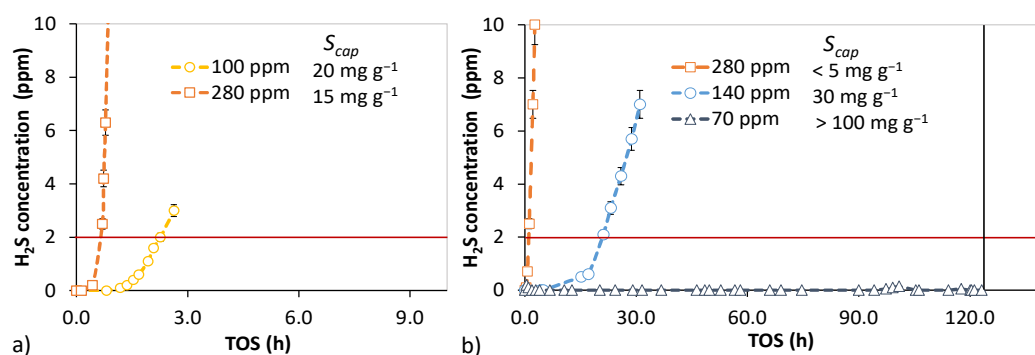


**Figure 3.** Effect of sulfur concentration on  $\text{H}_2\text{S}$  breakthrough in oxygen-containing and moist syngas. (a) IAC at SV  $24,000 \text{ h}^{-1}$  in reactor 1. Particle size distribution— $0.3\text{--}1.0 \text{ mm}$ . (b) Non-impregnated activated carbon (AC1) at SV  $3700 \text{ h}^{-1}$  in reactor 2. Particle size distribution— $1.0\text{--}1.25 \text{ mm}$ . A vertical black line indicates premature termination.

The  $\text{H}_2\text{S}$  concentration did not affect the capture capacity of IAC; however, at low space velocity (SV) for the AC1, the feed concentration played a key role. For non-impregnated activated carbons, major kinetic limitations are overcome at an  $\text{H}_2\text{S}$  concentration of 70 ppm. The contact time for gaseous  $\text{H}_2\text{S}$  and the carbon surface is sufficiently long for meaningful capture rates (the experiment was terminated before breakthrough at 120 h TOS). This setpoint equals a sulfur mass-based space velocity of  $0.8 \text{ mg (g}\cdot\text{h)}^{-1}$ .

Carbons modified by caustic chemicals such as KOH [33] and NaOH [34] or oxidative agents such as KI [11], like the IAC in this study, show reaction kinetics that are orders of magnitude faster and thus have higher adsorption efficiency compared to non-impregnated activated carbons [33]. Previously published results show that oxidation on non-impregnated carbon is rate-limited due to the complexity of the reactions steps [29,35]. Impregnation, however, does not necessarily increase the capture capacity. When the contact time between the gas and a non-impregnated activated carbon is long enough, sulfur capture can go to completion and the uptake is comparable to or even better than that with a modified carbon due to the large pore volume of non-impregnated carbon. Batch-type processes or applications where contact time is not crucial are thus more suitable for slow kinetics adsorption. For an industrially relevant  $\text{H}_2\text{S}$  removal process in continuous operation mode, fast reaction kinetics is a prerequisite.

Recently, doped activated carbons have emerged as an interesting alternative to impregnated carbons [36]. The relative performance of non-impregnated, impregnated, and doped activated carbons was tested at lab scale in the favorable conditions established in the previous section with oxygen and steam present in low  $\text{H}_2\text{S}$  concentration syngas. The results are visualized in Figure 4.

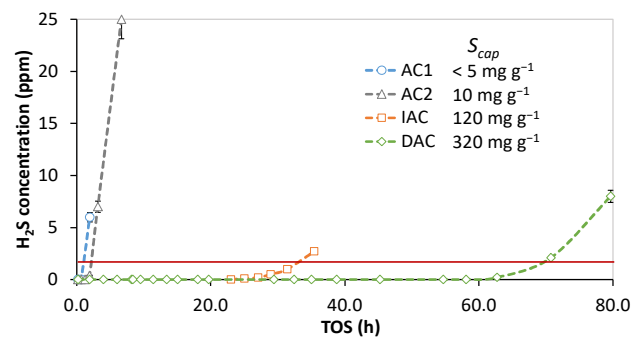


**Figure 4.** Relative sulfur capture capacity of activated carbon-based adsorbents in syngas with a feed of 70 ppm H<sub>2</sub>S, 3000 ppm oxygen, and 50% RH and SV 16,000 h<sup>-1</sup> (reactor 1). AC1 and AC2: non-impregnated activated carbon; IAC: impregnated activated carbon; DAC: doped activated carbon. Particle size distribution—0.5–0.85 mm.

The non-impregnated activated carbons AC1 and AC2 both performed poorly in the tested conditions due to their inherent limitations in the rate of adsorption. AC2, with its higher surface area and more developed microporosity, had a slightly longer breakthrough time. Generally, for the adsorption of small molecules, carbon with a high micropore volume is preferred, since the closer the pore width is to the adsorbate molecule, the stronger the adsorption force [22,31]. In the tested conditions, the impregnated carbon performed orders of magnitude better, with a capture capacity of 120 mg g<sup>-1</sup>. The best performance was achieved by the doped activated carbon (DAC), with a capture capacity of 320 mg g<sup>-1</sup>.

To put these results into context, Table 3 presents S<sub>cap</sub> results from previous fixed-bed H<sub>2</sub>S removal studies. The table features different types of activated carbons, commercial carbons, modified non-impregnated carbons, impregnated carbons, and doped carbons in inert, air, or biogas atmospheres.

**Table 3.** Low-temperature dynamic lab-scale H<sub>2</sub>S breakthrough capacities and the main operating conditions from previous studies.

AC	Gas	H <sub>2</sub> S (ppm)	O <sub>2</sub> (%)	RH (%)	T (°C)	SV	S <sub>cap</sub> -H <sub>2</sub> S (mg g <sup>-1</sup> )	Ref.
Non-impr. Na <sub>2</sub> CO <sub>3</sub> -impr.	N <sub>2</sub>	200	0	50	30	~2100 h <sup>-1</sup>	4 (C/C <sub>0</sub> = 0.25%) 13 (C/C <sub>0</sub> = 0.25%)	[12]
KI-impr. Non-impr.	He	3000	0	0	30	6000 cm <sup>3</sup> (g·h) <sup>-1</sup>	24 (C/C <sub>0</sub> = 10%) 17 (C/C <sub>0</sub> = 10%)	[37]
KOH-KI-impr. KOH-KI-impr.	Biogas	100	2 0	90 0	45	10,000 h <sup>-1</sup>	40 (C/C <sub>0</sub> = 50%) 24 (C/C <sub>0</sub> = 50%)	[16]
KOH-impr. KOH-impr.	Biogas	400	2	90	25	5000 h <sup>-1</sup> 15,000 h <sup>-1</sup>	130 (C/C <sub>0</sub> = 0.25%) 5 (C/C <sub>0</sub> = 0.25%)	[13]
Non-impr.	Biogas	-	0.3	0	20	~2700 h <sup>-1</sup>	4 (0.5 ppm limit)	[3]
Doped	Biogas	2000	0.4	50	50	R <sub>t</sub> : 2 s	~1000 (C/C <sub>0</sub> = 0.5%)	[36]
N-doped	Air	1000	21	80	25	5.5 g (g·h) <sup>-1</sup>	2770 (C/C <sub>0</sub> = 0.5%)	[38]
Non-impr. Cu-impr.	Air	3000	21	80	20	~7900 h <sup>-1</sup>	17 (C/C <sub>0</sub> = 3%) 490 (C/C <sub>0</sub> = 3%) (Partial conv. to SO <sub>2</sub> )	[39]
Melamine-impr.	Air	3000	21	80	25	~1300 h <sup>-1</sup>	250 (C/C <sub>0</sub> = 17%)	[40]
Non-impr.	Air	3000	21	80	25	~1300 h <sup>-1</sup>	290 (C/C <sub>0</sub> = 17%)	[41]

Since the capture capacity  $S_{cap}$  calculation is based on study-specific breakthrough limits, the values are not directly comparable with each other or values in this study. Nevertheless, the results show large disparities between capacities often caused by different operating conditions, especially  $H_2S$  feed concentration and space velocities. Generally, the reactor H/D ratio in this study is lower than in other studies, reflecting more realistic conditions with the cost of longer test duration. Special carbons such as nitrogen-species impregnated [40] or doped [36,38] variants or special formulated non-impregnated carbon [41] emerge as the best performing adsorbents for fixed-bed  $H_2S$  removal in oxygen-containing and moist gas. The oxygen and moisture content has a large positive effect on capture capacity for virtually all tested carbons, though it was shown by Barelli et al. [16] to not be as pronounced in biogas as in an inert atmosphere. In context of this study, desulfurization in a syngas atmosphere is shown to be especially sensitive to moisture and oxygen content. The exact mechanism for oxidation is still under debate, since studies have been performed with carbons with varying textural and surface species properties, which makes it difficult to achieve consensus on the matter. Proposed mechanisms for  $H_2S$  reactions on carbon defined by surface pH are summarized in Table 4.

**Table 4.**  $H_2S$  adsorption and reaction mechanisms of carbon surface defined by pH on activated carbon [20,34].

Surface pH	$H_2S$ Adsorption Mechanism	Reaction Mechanism and Final Product
>7	$H_2S$ chemisorption on $OH^-$ sites	$HS^-$ on water film and high $HS^-/O^*$ ratio leads to oxidation of solid S
4.5–7	Physical adsorption on wetted AC surfaces	Low $HS^-/O^*$ ratio results in $SO_x$ species which acidify and block pores in the form of $H_2SO_4$
<4.5	Physical adsorption on wetted AC surfaces	Strong $H_2SO_4$ formation, partial $H_2S$ redox with $H_2SO_4$ to form solid S

According to previously published studies, in low pH environments, only slow physical adsorption occurs. The low pH promotes the formation of hydrogen sulfide ions, which in the pores are partly converted to sulfuric acid. In basic conditions, fast chemisorption occurs and dissociation of  $H_2S$  to  $HS^-$  ions facilitates the oxidation of  $H_2S$  to elemental sulfur. Therefore, if a caustic material is present in oxygen containing conditions, oxidation to elemental sulfur is catalyzed until all of the base is exhausted [7,20,34]. Elemental sulfur in basic conditions forms polysulfides which in their stable form exist as sulfur polymers, such as  $S_8$ , with chain- or ring-like shapes [41,42]. All tested fresh adsorbents, AC1, AC2, and DAC, were basic, indicating fast chemisorption. With non-impregnated carbons, the surface oxide functional groups have been shown to be the active centers for oxidation [28].

Despite the benefits of impregnation of inorganic compounds, it presents several drawbacks. Impregnation lowers the available surface area by blocking pores and is in practice limited in  $H_2S$  uptake capacity relative to the impregnate amount [38]. In addition, the application of impregnates on carbons can lower the material self-ignition temperature, posing a safety hazard [42]. Impregnated carbons are also more expensive due to the additional processing requirement. A regeneration process would require re-applying the impregnate, which is more expensive than regeneration methods for non-impregnated carbons that are performed in situ. The regenerability also depends on the form of the sulfur deposits in the pores. Water-soluble compounds such as sulfuric acid can be efficiently washed away from the surface with minimal harm to the structure of the carbon [43]. Elemental sulfur in the form of bulky polymer chains is only partially removed by washing with water and thus requires more invasive methods for regeneration, including solvent extraction or thermal regeneration [7,37]. Bagreev et al. [44,45] showed that oxidation of a spent activated carbon sample in air at 300 °C converted all elemental

sulfur to  $\text{SO}_2$ , and a significant drop in sulfur capture capacity was also observed due to the changes in surface chemistry and porosity.

Doped activated carbons have emerged as an alternative to impregnated carbons and mitigate many of the downsides of impregnation. Doping differs from impregnation by mixing the dopant with the carbon precursor to achieve a more homogeneous distribution than with impregnation. As shown in Table 3,  $\text{H}_2\text{S}$  adsorption capacities above  $1 \text{ g g}^{-1}$  have been reported. Carbons with high  $\text{H}_2\text{S}$  uptake and faster reaction kinetics have been manufactured by incorporating heteroatoms such as oxygen or nitrogen into the carbon, which changes the acidic/basic character of the surface [40]. Especially interesting is nitrogen-group surface chemistry, where nitrogen-containing carbons enhance electron transfer reactions. Basic nitrogen-rich functional groups might be able to enhance the rate of dissociation of  $\text{H}_2\text{S}$  [23]. For nitrogen-doped activated carbons to be effective, both high surface density of active sites and high pore volume for sulfur deposition are needed [38]. Since the performance of DAC was the highest among tested carbons, DAC emerges as the best choice for syngas purification.

### 3.3. Ammonia-Enhanced $\text{H}_2\text{S}$ Oxidation

Only a few publications describe ammonia in terms of improving desulfurization performance. It is known that carbon surface treatment by ammonia can significantly improve  $\text{H}_2\text{S}$  removal, but this applies to all basic compounds in the adsorbent preparation stage [28]. An old study by Engelhardt [18] first mentioned the effect of gaseous ammonia for desulfurization on activated carbons, reporting a capture capacity over its own weight when oxygen and ammonia are injected into a gas stream. Turk et al. [19,46] reported similar findings showing that gaseous ammonia injection improved non-impregnated activated carbon desulfurization performance in air purification for wastewater treatment plants. A significant advantage over caustic activated carbons has been shown in both laboratory and pilot-plant results. Masuda et al. [47] tested the influence of ammonia on hydrogen sulfide and concluded that ammonia was not adsorbed at all, and its influence on desulfurization was too small to be evaluated, since the removal efficiency in the experiments was high even without ammonia. In an oxidation mechanism study by Li et al. [10], at  $150^\circ\text{C}$  adding ammonia to a model coke oven flue gas did not significantly improve desulfurization performance. Therefore, to further investigate the effect of gaseous ammonia on desulfurization, lab-scale breakthrough tests and spent adsorbent characterization were performed. The effect of ammonia on sulfur removal using non-impregnated activated carbon was tested in two space velocities in oxygen and steam containing syngas. The dynamic  $\text{H}_2\text{S}$  breakthrough results are shown in Figure 5.

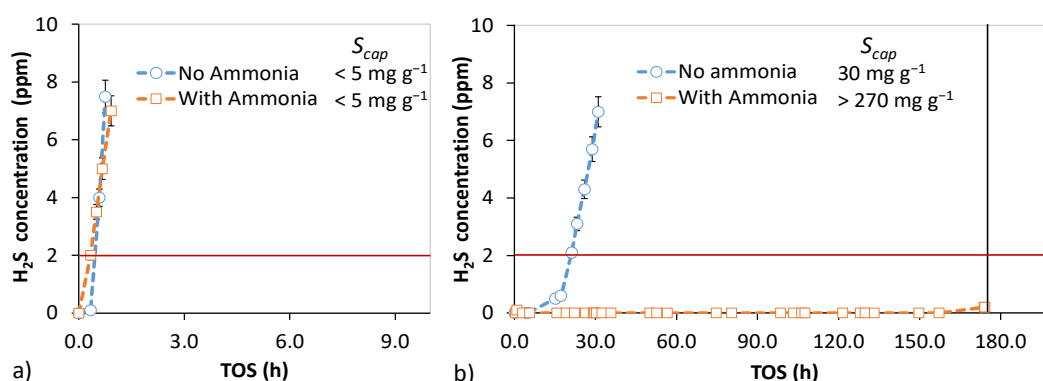
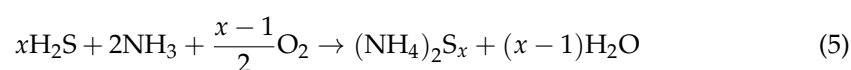


**Figure 5.** Effect of 35 ppm ammonia in syngas for  $\text{H}_2\text{S}$  removal using AC1 at  $50^\circ\text{C}$ . Syngas  $\text{O}_2$  concentration was 3000 ppm and RH was 50%. (a) SV  $16,000 \text{ h}^{-1}$  (reactor 1) and  $\text{H}_2\text{S}$  concentration 70 ppm. (b) SV  $3700 \text{ h}^{-1}$  (reactor 2) and  $\text{H}_2\text{S}$  concentration 140 ppm. Particle size distribution— $0.5\text{--}0.85 \text{ mm}$ .

At high SV, as shown in Figure 5a, adding ammonia to the gas stream did not affect sulfur uptake. However, at SV  $3700 \text{ h}^{-1}$  in Figure 5b a significant increase in capture

capacity could be observed in the ammonia-containing syngas. Due to the long test duration, a full 2 ppm breakthrough could not be completed. In the low SV breakthrough test of the ammonia-containing syngas, the top third of the bed showed signs of weak agglomeration of particles, which was not observed in other experiments. Figure 5b reflects realistic industrial conditions for adsorption/catalytic reactions, thus showing that ammonia enhancement is a potential method for low-H<sub>2</sub>S gas stream deep purification. Effective utilization of a high pore volume of non-impregnated activated carbons combined by improving the reaction kinetics without modifying the adsorbent material is very desirable, especially when ammonia is inherently present in many process gases. By carefully choosing the right reaction conditions to favor kinetically fast oxidation, untreated and thus cheaper adsorbent materials can be utilized.

Turk et al. [19] proposed two possible reaction pathways for explaining the effect of ammonia on sulfur capture. The first path forms ammonium polysulfide according to Reaction (5):



The second proposed path proceeds via multiple steps through intermediates NH<sub>4</sub>HS and NH<sub>4</sub>HSO<sub>3</sub> to form elemental sulfur with ammonia as the catalyst. Both mechanisms proceed by oxidation, and the difference is that in the ammonium polysulfide pathway, ammonia is a reactant. They determined the NH<sub>3</sub>-to-S ratio by titration to be around 25, therefore corresponding to an *x* value of approximately 50 in Reaction (5) [19]. To investigate if ammonia was consumed in the reaction in this study, ammonia breakthrough curves from the experiments shown in Figure 5 were graphed, as shown in Figure 6.

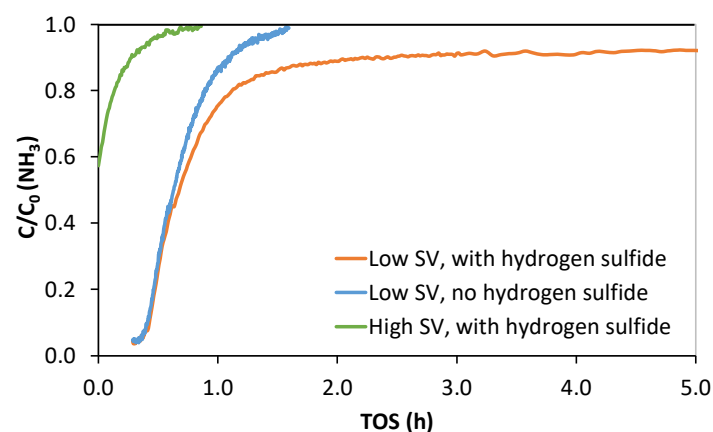


**Figure 6.** Continuous Fourier transform infrared spectroscopy (FTIR) measurement results of ammonia concentration for the experiments shown in Figure 5. The green line indicates the experiment conducted in reactor 1 and blue and orange lines in reactor 2. Ammonia feed concentration—35 ppm. The blue line indicates a control experiment conducted in syngas without H<sub>2</sub>S.

At high SV, NH<sub>3</sub> breakthrough is instantaneous and complete, not unlike with H<sub>2</sub>S, while for low SV an interesting discrepancy in breakthrough behavior is observed. The control experiment without H<sub>2</sub>S in feed reached full ammonia breakthrough, while the experiment with ammonia with high sulfur capture capacity reached a steady state of  $C/C_0 \sim 0.95$  (Figure 6 displays the first 5 h on stream). Full ammonia breakthrough was not observed during the 175 h time on stream. Since the AC1 surface pH was high, any physical ammonia adsorption would be very weak. These results indicate that a few ppm of ammonia is consumed in the carbon bed and that the ammonium polysulfide reaction mechanism may be valid.

The spent samples from the experiments shown in Figure 5 were further characterized, and the weight change results from thermal analysis in inert gas are presented Figure 7a. Pore volume change as a function of pore width was obtained with N<sub>2</sub> adsorption/desorption tests, visualized in Figure 7b.

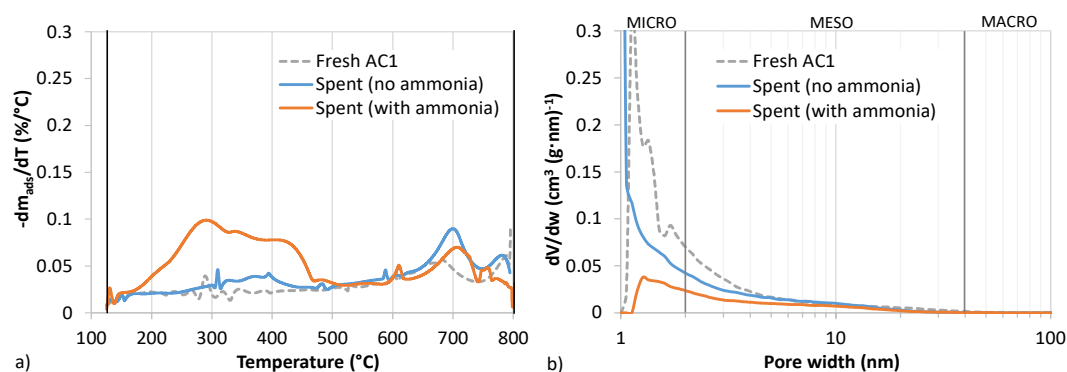


**Figure 7.** Characterization of fresh and spent AC1 from experiments with and without ammonia in syngas as presented in Figure 5b. (a) Thermogravimetric analysis (TGA) in  $N_2$ . Percentage weight change derivative (weight loss) as a function of temperature. (b) Pore volume change as a function of pore width.

In Figure 7a thermal analysis of the spent sample from the experiment with ammonia shows between 200 and 450 °C (maximum at 290 °C) weight loss above the fresh adsorbent baseline, which is attributed to sulfur vaporization. The baseline subtracted weight loss equals ca. 12% sulfur loading in the sample. The breakthrough test bed mass increased 31%, which is agreement with the theoretical sulfur mass flow during the experiment. This indicates that some of the bound sulfur was not released in the range 125–500 °C. The sample from the experiment without ammonia only shows a slightly elevated weight loss compared to baseline in the range 300–400 °C. In theory, elemental sulfur in ring form,  $S_8$ , has a boiling point of 444 °C [43]. However, previous studies, which investigated the volatilization temperatures of sulfur species on carbons, attributed release of elemental sulfur to occur at 250–400 °C. Oxidised compounds from e.g. sulfuric acid decomposition or  $SO_2$  release occurs at lower temperatures of 150–250 °C. [23,39] Both spent adsorbents thus likely contained sulfur in elemental form confirming that oxidation of  $H_2S$  occurred.

From Figure 7b, it can be seen that the pore volume distribution changed considerably after the breakthrough test. The specific surface area of the spent adsorbent from the ammonia experiment decreased from 520 to 110  $m^2 g^{-1}$ . For the spent adsorbent in the ammonia-free atmosphere, the sulfur was deposited to the mesopores, while the micropore volume remained unchanged. With the ammonia sample, the micropore volume was almost completely exhausted, and the mesopore volume was significantly reduced. If the reaction proceeds to form long-chained ammonium polysulfides, then the molecular size alone would dictate that they deposit in the larger pores. The results, however, are consistent with studies by Bandosz et al. [23] demonstrating that active centers exist primarily in micropores where strongly bound sulfur favorably deposits. The aggregate micro- and mesopore volumes as well as specific surface areas and bed mass changes along with measured surface pH for the three samples are reported in Table 5.

**Table 5.** Spent adsorbent characterization from lab-scale experiments presented in Figure 5b (SV 3700  $h^{-1}$ ).

	Fresh		Spent	
	AC1	No Ammonia	With Ammonia	
Bed Mass Change (%)		4	31	
pH	10.8	9.4	8.0	
EDS Surface Analysis (%): Sulfur <sup>1</sup>	1.3 ± 0.3	3.7 ± 2.0	18.8 ± 5.5	

<sup>1</sup> Average sample results for six randomly chosen particles presented with standard deviations. Results in mass fractions.

The bed mass increase indicates that  $H_2S$  was fully captured in carbon pores and any significant  $SO_2$  or COS formation was therefore effectively ruled out. A 2 h experiment

with AC2 in syngas atmosphere without H<sub>2</sub>S was used to verify that bed mass increase was not caused by adsorption of other compounds. The surface pH measurement is consistent with the other results. Spent adsorbent pH decreased from the fresh AC1 sample, which had a basic pH of 10.8. Since the ammonia breakthrough time was longer, more sulfur was captured, leading to a lower pH.

The particle surface elemental composition derived from EDS analysis showed that the sulfur content in the ammonia-free experiment was slightly higher than in the fresh sample. The sample from the ammonia experiment showed high sulfur loading at an average of 18.8%.

### 3.4. Bench-Scale Desulfurization

To assess the efficacy of activated carbons for real syngas desulfurization, bench-scale sulfur removal in a gasification slipstream was performed. The day-long experiments were operated at a high space velocity to accelerate breakthrough. The breakthrough results are shown in Figure 8.

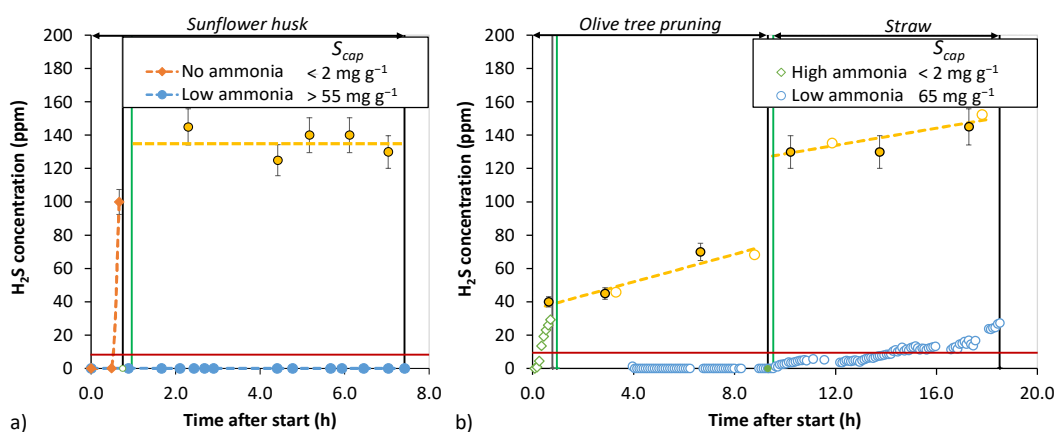


**Figure 8.** High space velocity ( $\sim 15,500\text{--}17,500\text{ h}^{-1}$ ) bench-scale H<sub>2</sub>S breakthrough experiments. (a) One day campaign with adsorbent AC2 with sunflower husk-based syngas. Syngas feed H<sub>2</sub>S content rate—125–150 ppm. (b) Two-day campaign with adsorbent AC1 in olive tree pruning- and straw-based syngas. Particle size distribution—1.0–1.25 mm. Vertical green lines indicate start, and black lines indicate the end of the experiment. Experiments were performed at atmospheric pressure and 16–18 °C temperature. Hollow markers: GC analysis; filled markers: Dräger analysis. Yellow dashed line indicates estimated feed H<sub>2</sub>S concentration.

In Figure 8a the AC2 experiment with partial NH<sub>3</sub> breakthrough (NH<sub>3</sub> content not quantified) resulted in effective H<sub>2</sub>S removal on the carbon (dashed blue line), while in the first setpoint with ammonia-free syngas, an almost instantaneous and sharp breakthrough occurred (dashed orange line). In the two-day campaign experiment, the H<sub>2</sub>S feed concentration varied more. In Figure 8b, the first setpoint with instantaneous H<sub>2</sub>S breakthrough for AC1 with high ammonia concentration was observed despite the low H<sub>2</sub>S feed concentration. This indicates that a high ammonia concentration in the syngas interferes with H<sub>2</sub>S oxidation. The ammonia analysis for the syngas showed a high concentration of 760 ppm. Following this, partial NH<sub>3</sub> removal was reinstated and H<sub>2</sub>S removal was again effective. For partial ammonia breakthrough, analysis showed for the olive tree feedstock 13 ppm (6 h after start) and for the straw 25 ppm (18 h after start) ammonia concentration in the gas. The breakthrough capacity was around 65 mg g<sup>-1</sup> and the total loading was 100 mg g<sup>-1</sup>, indicating that even a low ammonia-to-H<sub>2</sub>S ratio of 0.15–0.25 is sufficient for enhancing the adsorption kinetics. COS concentration in the raw syngas was in the range of 5–35 ppm, and the results indicated that the activated carbon bed did not capture any COS or convert H<sub>2</sub>S to COS or SO<sub>2</sub> during the course of the whole two-day campaign.

The spent AC1 was analyzed for specific surface area and pore volume for three bed depths: surface, middle, and bottom. The results are reported in Table 6.

**Table 6.** Spent adsorbent characterization from bench-scale experiments presented in Figure 8b.

	Fresh	Spent		
	AC1	Top	Middle	Bottom
N <sub>2</sub> adsorption/desorption analysis <sup>1</sup>				
BET-SA (m <sup>2</sup> g <sup>-1</sup> )	520	140	230	330
V <sub>mic</sub> (cm <sup>3</sup> g <sup>-1</sup> )	0.13	0	0.04	0.07
V <sub>mes</sub> (cm <sup>3</sup> g <sup>-1</sup> )	0.28	0.21	0.17	0.23
Ultimate analysis (%) <sup>2</sup>				
C	66.2 ± 1.6	57.8 ± 1.2	55.4 ± 1.3	62.1 ± 2.3
H	0.5 ± 0.0	0.6 ± 0.1	0.6 ± 0.0	0.6 ± 0.1
N	0.5 ± 0.1	0.4 ± 0.0	0.4 ± 0.0	0.4 ± 0.1
S	1.0 ± 0.1	16.0 ± 0.2	11.1 ± 0.3	7.0 ± 0.5

<sup>1</sup> Spent bed samples: random selection from each bed layer. <sup>2</sup> Spent bed samples: random selection from each bed layer. Average mass-based result of three samples presented with standard deviation.

The surface layer microporosity was completely lost. The BET-SA was 140 m<sup>2</sup> g<sup>-1</sup>, while for the middle layer it was 230 m<sup>2</sup> g<sup>-1</sup>, and the bottom layer 330 m<sup>2</sup> g<sup>-1</sup>. This confirms that the H<sub>2</sub>S deposits primarily in the micropores, which explains the (likely) better H<sub>2</sub>S capacity of AC1 in the bench-scale tests, since it has higher available micropore volume. The elemental analysis showed that the sulfur content decreased along the bed depth, with 16 % by mass in the top third, while the bottom third sulfur content was on average 7 %. No sign of increase in nitrogen content in the spent samples can be observed.

#### 4. Discussion

Based on the lab- and bench-scale results and authors' assessments, a qualitative comparison for activated carbons suitable for H<sub>2</sub>S removal from syngas is presented in Table 7.

**Table 7.** Comparison of standard AC, ammonia-enhanced AC, impregnated AC and doped AC for low-temperature syngas H<sub>2</sub>S removal. Favorable characteristics are indicated with the ++/+ sign and the—sign for unfavorable characteristics.

Adsorbent Properties	AC	AC (NH <sub>3</sub> Enhanced)	Impregnated AC	Doped AC
Capture capacity	+	++	+	++
Capture rate	—	++	+	++
Removal level	++	++	++	++
Selectivity	—	—	—	—
Regenerability	+	—	—	—
Safety and environment	+	+	—	+
Cost	++	++	+	—

All of the options mentioned in Table 7 require an oxygen-containing atmosphere with moisture to facilitate the oxidation reaction for improved sulfur capture rate. The equilibrium capture capacity for activated carbons is assessed to be high on a mass-basis relative to other available adsorbents, but volume-based capacity suffers from their inherent low density [48,49]. The adsorption rates exhibited in this study show that H<sub>2</sub>S removal is feasible to high purity levels at industrially relevant conditions with ammonia-enhanced AC, IAC, and DAC. Activated carbons are in general non-selective, which can be an issue in a multicontaminant gas. The regenerability of activated carbons is not evaluated in this paper, but it was assumed for the comparison that physically adsorbed sulfur is easy to regenerate relative to chemically adsorbed sulfur species. Non-impregnated carbons are assumed to be the least expensive, with increasing cost from additional complexity for impregnated and doped carbons. Ammonia-enhanced oxidation on carbon compares

favorably to the other activated carbon options, though the same inherent unfavorable characteristics that activated carbons in general possess are still present.

The bench-scale breakthrough experiments in real syngas validate the effectiveness of ammonia-enhanced desulfurization that was established in the lab-scale tests. Ammonia enhancement upgrades non-impregnated activated carbons to operate on par with the best available modified activated carbons for high-capacity deep desulfurization. The main downsides of this method are the additional cost of potential ammonia concentration control upstream and the added complexity of removing the excess ammonia downstream. Ammonia is a polar and basic compound that could, in low concentrations, feasibly be removed for high gas purity applications by activated carbons directly after the sulfur removal of the AC bed. Carbons that exhibit acidic sites or carbons with impregnates such as mineral acids could be utilized [50]. Adsorption capacities of up to 140 mg ammonia per gram of activated carbon have been reported in literature [51]. Low-temperature oxidative H<sub>2</sub>S removal processes are also burdened by the possible downstream removal of oxygen. The possibility of regenerating the ammonia-enhanced activated carbon would also affect the viability of the method. There are, however, claims that regeneration of the spent activated carbon bed using solvent extraction would be possible [18].

## 5. Conclusions

The lab-scale fixed-bed H<sub>2</sub>S breakthrough test in syngas verified previous findings that for activated carbons, H<sub>2</sub>S removal was markedly improved when moisture and oxygen were added. This is due to low-temperature selective oxidation of H<sub>2</sub>S to form elemental sulfur, which improves the sulfur uptake rate compared with purely physical adsorption. The best sulfur capture performance was achieved by doped activated carbon at 320 mg g<sup>-1</sup>, followed by KI impregnated carbon at 120 mg g<sup>-1</sup>. Ammonia was shown to significantly affect the sulfur uptake rate of non-impregnated activated carbon. Especially in breakthrough tests with lower space velocity, a significant increase in capture capacity to  $\geq 270$  mg g<sup>-1</sup> and an exhaustion of the micropore volume was observed. Continuous effluent analysis revealed that a small quantity of ammonia was captured or consumed by the carbon bed. This indicates that the reaction mechanism in which ammonium polysulfide is formed, as proposed by Turk et al. [19], may be valid. In real gasification syngas experiments at bench-scale, when ammonia was present at low concentrations (tens of ppm), H<sub>2</sub>S oxidation proceeded rapidly. With high ammonia feed concentrations (hundreds of ppm), instantaneous H<sub>2</sub>S breakthrough occurred, similar to ammonia-free syngas. It was established that the ability to utilize cheaper non-impregnated activated carbons by in situ enhancement of the adsorption kinetics without modifying the adsorbent material is very desirable, especially when ammonia is inherently present in many process gases. Ammonia enhancement is therefore a viable route for high-capacity process gas H<sub>2</sub>S adsorption, essentially realizing full utilization of virgin carbon pore volume and therefore allowing practical application of non-impregnated carbons in continuous processes.

**Author Contributions:** Conceptualization C.F. and I.H.; data curation, C.F.; formal analysis, C.F.; funding acquisition, P.S.; investigation and methodology, C.F., I.H., and P.S.; project administration, P.S.; supervision, P.S. and I.H.; writing—original draft, C.F.; writing—review and editing, P.S. All authors have read and agreed to the published version of the manuscript.

**Funding:** This research was funded by the European Union's Horizon 2020 research and innovation program, COMSYN project, grant number 727476, and the BioSFerA project, grant number 884208.

**Institutional Review Board Statement:** Not applicable.

**Informed Consent Statement:** Not applicable.

**Data Availability Statement:** Not applicable.

**Acknowledgments:** The authors would like to thank the laboratory staff for their contributions: Petri Hietula, Patrik Eskelinen, and Mirja Muhola.

**Conflicts of Interest:** The authors declare no conflict of interest.

### Abbreviations

AC	Activated carbon
BJH	Barrett–Joyner–Halenda
DAC	Doped activated carbon
EDS	Energy dispersive X-ray spectroscopy
FPD	Flame photometric detector
FTIR	Fourier-transform infrared spectroscopy
IAC	Impregnated activated carbon
n.a.	Not analyzed
RH	Relative humidity
$R_t$	Residence time
SA	Surface area
Scap	Sulfur adsorption capacity
SEM	Scanning electron microscope
SV	Space velocity (volumetric)
TCD	Thermal conductivity detector
TOS	Time on stream
w	Pore width

### References

1. Shah, M.S.; Tsapatsis, M.; Siepmann, J.I. Hydrogen Sulfide Capture: From Absorption in Polar Liquids to Oxide, Zeolite, and Metal-Organic Framework Adsorbents and Membranes. *Chem. Rev.* **2017**, *117*, 9755–9803. [[CrossRef](#)]
2. Benedetti, V.; Patuzzi, F.; Baratieri, M. Gasification Char as a Potential Substitute of Activated Carbon in Adsorption Applications. *Energy Procedia* **2017**, *105*, 712–717. [[CrossRef](#)]
3. Coppola, G.; Papurello, D. Biogas Cleaning: Activated Carbon Regeneration for H<sub>2</sub>S Removal. *Clean Technol.* **2018**, *1*, 40–57. [[CrossRef](#)]
4. Nakamura, S.; Kitano, S.; Yoshikawa, K. Biomass gasification process with the tar removal technologies utilizing bio-oil scrubber and char bed. *Appl. Energy* **2016**, *170*, 186–192. [[CrossRef](#)]
5. Sisani, E.; Cinti, G.; Discepoli, G.; Penchini, D.; Desideri, U.; Marmottini, F. Adsorptive removal of H<sub>2</sub>S in biogas conditions for high temperature fuel cell systems. *Int. J. Hydrogen Energy* **2014**, *39*, 21753–21766. [[CrossRef](#)]
6. Wang, S.; Nam, H.; Nam, H. Preparation of activated carbon from peanut shell with KOH activation and its application for H<sub>2</sub>S adsorption in confined space. *J. Environ. Chem. Eng.* **2020**, *8*, 103683. [[CrossRef](#)]
7. Bagreev, A.; Rahman, H.; Bandoz, T.J. Study of H<sub>2</sub>S adsorption and water regeneration of spent coconut-based activated carbon. *Environ. Sci. Technol.* **2000**, *34*, 4587–4592. [[CrossRef](#)]
8. Le Leuch, L.M.; Subrenat, A.; Le Cloirec, P. Hydrogen sulfide adsorption and oxidation onto activated carbon cloths: Applications to odorous gaseous emission treatments. *Langmuir* **2003**, *19*, 10869–10877. [[CrossRef](#)]
9. Habeeb, O.A.; Ramesh, K.; Goma, A.M.; Ali, G.A.M.; Yunus, R.M.; Thanusha, T.K.; Olalere, O.A. Modeling and Optimization for H<sub>2</sub>S Adsorption from Wastewater Using Coconut Shell Based Activated Carbon. *Aust. J. Basic Appl. Sci.* **2016**, *10*, 136–147.
10. Li, Y.; Lin, Y.; Xu, Z.; Wang, B.; Zhu, T. Oxidation mechanisms of H<sub>2</sub>S by oxygen and oxygen-containing functional groups on activated carbon. *Fuel Process. Technol.* **2019**, *189*, 110–119. [[CrossRef](#)]
11. Choi, D.-Y.; Lee, J.; Jang, S.; Ahn, B.; Choi, D. Adsorption dynamics of hydrogen sulfide in impregnated activated carbon bed. *Adsorption* **2008**, *14*, 533–538. [[CrossRef](#)]
12. Xiao, Y.; Wang, S.; Wu, D.; Yuan, Q. Experimental and simulation study of hydrogen sulfide adsorption on impregnated activated carbon under anaerobic conditions. *J. Hazard. Mater.* **2008**, *153*, 1193–1200. [[CrossRef](#)]
13. Isik-Gulsac, I. Investigation of impregnated activated carbon properties used in hydrogen sulfide fine removal. *Brazilian J. Chem. Eng.* **2016**, *33*, 1021–1030. [[CrossRef](#)]
14. Guo, J.; Luo, Y.; Chong Lua, A.; Chi, R.A.; Chen, Y.; Bao, X.; Xiang, S. Adsorption of hydrogen sulphide (H<sub>2</sub>S) by activated carbons derived from oil-palm shell. *Carbon N. Y.* **2007**, *45*, 330–336. [[CrossRef](#)]
15. Feng, W.; Kwon, S. Adsorption of Hydrogen Sulfide onto Activated Carbon Fibers: Effect of Pore Structure and Surface Chemistry. *Environ. Sci. Technol.* **2005**, *39*, 9744–9749. [[CrossRef](#)] [[PubMed](#)]
16. Barelli, L.; Bidini, G.; de Arespacochaga, N.; Pérez, L.; Sisani, E. Biogas use in high temperature fuel cells: Enhancement of KOH-KI activated carbon performance toward H<sub>2</sub>S removal. *Int. J. Hydrogen Energy* **2017**, *42*, 10341–10353. [[CrossRef](#)]
17. Georgiadis, A.G.; Charisiou, N.D.; Goula, M.A. Removal of Hydrogen Sulfide From Various Industrial Gases: A Review of The Most Promising Adsorbing Materials. *Catalysts* **2020**, *10*, 521. [[CrossRef](#)]
18. Engelhardt, A. Sulphur recovery and gas purification. Conversion of hydrogen sulphide into sulphur by means of activated charcoal. *Z. Angew. Chem.* **1921**, *34*, 293–295. [[CrossRef](#)]

19. Turk, A.; Sakalis, E.; Lessuck, J.; Karamitsos, H.; Rago, O. Ammonia injection enhances capacity of activated carbon for hydrogen sulfide and methyl mercaptan. *Environ. Sci. Technol.* **1989**, *23*, 1242–1245. [[CrossRef](#)]
20. Frilund, C.; Tuomi, S.; Kurkela, E.; Simell, P. Small- to medium-scale deep syngas purification: Biomass-to-liquids multi-contaminant removal demonstration. *Biomass Bioenergy* **2021**, *148*, 10. [[CrossRef](#)]
21. Frilund, C.; Simell, P.; Kurkela, E.; Eskelinen, P. Experimental Bench-Scale Study of Residual Biomass Syngas Desulfurization Using ZnO-Based Adsorbents. *Energy Fuels* **2020**, *34*, 3326–3335. [[CrossRef](#)]
22. Thommes, M.; Kaneko, K.; Neimark, A.V.; Olivier, J.P.; Rodriguez-Reinoso, F.; Rouquerol, J.; Sing, K.S.W. Physisorption of gases, with special reference to the evaluation of surface area and pore size distribution (IUPAC Technical Report). *Pure Appl. Chem.* **2015**, *87*, 1051–1069. [[CrossRef](#)]
23. Bandosz, T.J. On the adsorption/oxidation of hydrogen sulfide on activated carbons at ambient temperatures. *J. Colloid Interface Sci.* **2002**, *246*, 1–20. [[CrossRef](#)]
24. Li, Q.; Lancaster, J.R. Chemical foundations of hydrogen sulfide biology. *Nitric Oxide Biol. Chem.* **2013**, *35*, 21–34. [[CrossRef](#)] [[PubMed](#)]
25. Zhang, X.; Tang, Y.; Qu, S.; Da, J.; Hao, Z. H<sub>2</sub>S-Selective Catalytic Oxidation: Catalysts and Processes. *ACS Catal.* **2015**, *1067*, 1053–1067. [[CrossRef](#)]
26. Wu, X.; Schwartz, V.; Overbury, S.H.; Armstrong, T.R. Desulfurization of Gaseous Fuels Using Activated Carbons as Catalysts for the Selective Oxidation of Hydrogen Sulfide. *Energy Fuels* **2005**, *19*, 1774–1782. [[CrossRef](#)]
27. Gardner, T.H.; Berry, D.A.; Lyons, K.D.; Beer, S.K.; Freed, A.D. Fuel processor integrated H<sub>2</sub>S catalytic partial oxidation technology for sulfur removal in fuel cell power plants. *Fuel* **2002**, *81*, 2157–2166. [[CrossRef](#)]
28. Steijns, M.; Mars, P. The Role Partial of Sulfur Oxidation Trapped in Micropores of Hydrogen Sulfide in the Catalytic with Oxygen. *J. Catal.* **1974**, *35*, 11–17. [[CrossRef](#)]
29. Steijns, M.; Derks, F.; Verloop, A.; Mars, P. The Mechanism of the Catalytic Oxidation of Hydrogen Sulfide II. *J. Catal.* **1976**, *42*, 87–95. [[CrossRef](#)]
30. Dalai, A.K.; Tollefson, E.L. Kinetics and reaction mechanism of catalytic oxidation of low concentrations of hydrogen sulfide in natural gas over activated carbon. *Can. J. Chem. Eng.* **1998**, *76*, 902–914. [[CrossRef](#)]
31. Bansal, R.C.; Goyal, M. *Activated Carbon Adsorption*; Taylor & Francis: Boca Raton, FL, USA, 2005; ISBN 9780824753443.
32. Meeyoo, V.; Trimm, D.L.; Cant, N.W. Adsorption-reaction processes for the removal of hydrogen sulphide from gas streams. *J. Chem. Technol. Biotechnol.* **1997**, *68*, 411–416. [[CrossRef](#)]
33. Yan, R.; Liang, D.T.; Tsen, L.; Tay, J.H. Kinetics and mechanisms of H<sub>2</sub>S adsorption by alkaline activated carbon. *Environ. Sci. Technol.* **2002**, *36*, 4460–4466. [[CrossRef](#)] [[PubMed](#)]
34. Bashkova, S.; Armstrong, T.R.; Schwartz, V. Selective catalytic oxidation of hydrogen sulfide on activated carbons impregnated with sodium hydroxide. *Energy Fuels* **2009**, *23*, 1674–1682. [[CrossRef](#)]
35. Bandosz, T.J.; Bagreev, A.; Adib, F.; Turk, A. Unmodified versus caustics-impregnated carbons for control of hydrogen sulfide emissions from sewage treatment plants. *Environ. Sci. Technol.* **2000**, *34*, 1069–1074. [[CrossRef](#)]
36. Rossow, S.; Deerber, G.; Goetze, T.; Kanswohl, N.; Nelles, M. Biogas desulfurization with doped activated carbon. *Landtechnik* **2009**, *3*, 202–205.
37. Sitthikhankaew, R.; Chadwick, D.; Assabumrungrat, S. Effect of KI and KOH Impregnations over Activated Carbon on H<sub>2</sub>S Adsorption Performance at Low and High Temperatures. *Sep. Sci. Technol.* **2014**, *49*, 354–366. [[CrossRef](#)]
38. Sun, F.; Liu, J.; Chen, H.; Zhang, Z.; Qiao, W.; Long, D.; Ling, L. Nitrogen-rich mesoporous carbons: Highly efficient, regenerable metal-free catalysts for low-temperature oxidation of H<sub>2</sub>S. *ACS Catal.* **2013**, *3*, 862–870. [[CrossRef](#)]
39. Nguyen-Thanh, D.; Bandosz, T.J. Activated carbons with metal containing bentonite binders as adsorbents of hydrogen sulfide. *Carbon N. Y.* **2005**, *43*, 359–367. [[CrossRef](#)]
40. Bagreev, A.; Menendez, J.A.; Dukhno, I.; Tarasenko, Y.; Bandosz, T.J. Bituminous coal-based activated carbons modified with nitrogen as adsorbents of hydrogen sulfide. *Carbon N. Y.* **2004**, *42*, 469–476. [[CrossRef](#)]
41. Adib, F.; Bagreev, A.; Bandosz, T.J. Effect of pH and surface chemistry on the mechanism of H<sub>2</sub>S removal by activated carbons. *J. Colloid Interface Sci.* **1999**, *216*, 360–369. [[CrossRef](#)]
42. Yan, R.; Chin, T. Influence of Surface Properties on the Mechanism of H<sub>2</sub>S Removal by Alkaline Activated Carbons. *Environ. Sci. Technol.* **2004**, *38*, 316–323. [[CrossRef](#)]
43. Adib, F.; Bagreev, A.; Bandosz, T.J. On the possibility of water regeneration of unimpregnated activated carbons used as hydrogen sulfide adsorbents. *Ind. Eng. Chem. Res.* **2000**, *39*, 2439–2446. [[CrossRef](#)]
44. Bagreev, A.; Rahman, H.; Bandosz, T.J. Study of regeneration of activated carbons used as H<sub>2</sub>S adsorbents in water treatment plants. *Adv. Environ. Res.* **2002**, *6*, 303–311. [[CrossRef](#)]
45. Bagreev, A.; Rahman, H.; Bandosz, T.J. Thermal regeneration of a spent activated carbon previously used as hydrogen sulfide adsorbent. *Carbon N. Y.* **2001**, *39*, 1319–1326. [[CrossRef](#)]
46. Turk, A.; Mahmood, K.; Mozaffari, J. Activated Carbon For Air Purification In New York City's Sewage Treatment Plants. *Wat. Sci. Tech.* **1993**, *27*, 121–126. [[CrossRef](#)]
47. Masuda, J.; Fukuyama, J.; Fujii, S. Influence of concurrent substances on removal of hydrogen sulfide by activated carbon. *Chemosphere* **1999**, *39*, 1611–1616. [[CrossRef](#)]

48. Vaziri, R.S.; Babler, M.U. Removal of hydrogen sulfide with metal oxides in packed bed reactors-A review from a modeling perspective with practical implications. *Appl. Sci.* **2019**, *9*. [[CrossRef](#)]
49. Frilund, C.; Simell, P.; Kaisalo, N.; Kurkela, E.; Koskinen-Soivi, M.-L. Desulfurization of Biomass Syngas Using ZnO-Based Adsorbents: Long-Term Hydrogen Sulfide Breakthrough Experiments. *Energy Fuels* **2020**, *34*, 3316–3325. [[CrossRef](#)] [[PubMed](#)]
50. Rodrigues, C.C.; de Moraes, D.; da Nóbrega, S.W.; Barboza, M.G. Ammonia adsorption in a fixed bed of activated carbon. *Bioresour. Technol.* **2007**, *98*, 886–891. [[CrossRef](#)]
51. Guo, J.; Xu, W.S.; Chen, Y.L.; Lua, A.C. Adsorption of NH<sub>3</sub> onto activated carbon prepared from palm shells impregnated with H<sub>2</sub>SO<sub>4</sub>. *J. Colloid Interface Sci.* **2005**, *281*, 285–290. [[CrossRef](#)]